Electronic Supplementary Information

Supplementary Information

Chemical-mechanical coupling effect induced by charge distribution engineering enables long-lived phosphorous anode for lithium-ion batteries

*Weiqiang Kong[1], Wenruo Li[1], Wenhao Yu, Haoyuan Zhu, Shaofeng Xu, Shun Liu, Liying Cui and Zhongsheng Wen**

Department of Materials, Dalian Maritime University, Dalian 116026, China

E-mail: zswen5@gmail.com

Experimental Section

Synthesis of CoPPc: Typically, 4.10g urea, 1.00g NH_4Cl, 1.20g $CoCl_2 \cdot 6H_2O$, 0.025g $(NH_4)_6Mo_7O_{24} \cdot 4H_2O$, 1.74g pyromellitic dianhydride and a certain amount of edge blocking agent were mixed and ground in an agate mortar thoroughly. Thereinto, the mole ratio of pyromellitic dianhydride and edge blocking agent was determined to be 4:1. Besides, the as-prepared mixed materials were transferred into a drying oven for heat treatment at 220 °C for 3h under a heating rate of 5 ℃ min^{-1}. Then the obtained products were washed several times with H_2O, ethanol, tetrahydrofuran for several times to purify. Afterwards, the precipitates were dried at 70 ℃ overnight in a vacuum oven. Finally, the dry products were collected and ground into powder. The CoPPc powder was obtained successfully.

Synthesis of P, P/CoPPc and P-CoPPc/GO: The P/CoPPc and P-CoPPc/GO composites were prepared by a simple method of ball-milling. For detail, the red phosphorus and CoPPc were hand-milled together for 10 minutes in a mortar with a mass ratio of 7:3. Subsequently, the mixture was transferred into a stainless-steel jar and sealed under argon atmosphere in glovebox. The ratio mass of steel balls to raw materials is approximately 60:1. The condition of ball-milling process was the speed of 480 rpm for 10 h. In the end, the P/CoPPc composite was synthesized successfully. The P-CoPPc/GO composite was prepared by a two-step ball-milling method, where the mass ratio of the aforementioned

P/CoPPc composite to GO was 7:3. First of all, the P/CoPPc composite and GO were also mixed and ground in a mortar. Furthermore, the P-CoPPc/GO composite was prepared by mechanical ball milling under the same conditions. For comparison, the P material was obtained by the same method. In addition, we prepared the red phosphorus/CoPPc and red phosphorus/CoPPc/GO materials by manual grinding, respectively (Recorded as M-P/CoPPc and M-P-CoPPc/GO).

Material characterizations: The crystalline structures of all samples were analyzed by means of an X-ray powder diffraction (XRD) diffractometer (Rigaku D/max-3A) with Co Kα radiation (λ = 1.79 Å) and the scanning range 2θ from 10° to 90°. And the scanning rate speed is chosen as 8° min^{-1}. Scanning electron microscopy (SEM) and corresponding energy dispersive spectroscopy (EDS) mapping were carried out on SUPER55 /SAPPHIRE. The high-resolution transmission electron microscopy (HRTEM) was performed on JEM-2100 instrument to further characterize the morphology of P-CoPPc/GO composites. The X-ray photoelectron spectrometer (XPS) system (K-Alpha 1063) was employed to investigate valence states of P, Co, N, C and O elements of CoPPc, P/CoPPc and P-CoPPc/GO composites.

Electrochemical measurements: The working electrodes were prepared by mixing the 60 wt% active materials (P, P/CoPPc and P-CoPPc/GO), 20 wt% carbon black and 20 wt% polyvinylidene difluorides (PVDF). And the 1-methyl-2-pyrrolidinone (NMP) was used as the solvent to make above materials into a homogeneous slurry by ball-milling method. Subsequently, the slurry was uniformly coated on the copper foil and dried in a vacuum oven of 80 °C for 10h. And the dried copper foil is cut into evenly sized electrodes by machine for batteries fabrication. The CR2025 coin half cells were assembled in an Ar-filled glove box to conduct the electrochemical tests of the P, P/CoPPc and P-CoPPc/GO composites with the lithium metal as the counter electrodes. The commercial electrolyte was composed of 1.0 M $LiPF_6$ dissolved in the solvent of ethylene carbonate/ethyl methyl carbonate/dimethyl carbonate (EC/EMC/DMC=1:1:1, vol%). All the cells were tested under ambient temperature and placed to ensure that the electrodes were completely soaked by electrolyte before electrochemical measurement. The galvanostatic charge/discharge and rate measurements were conducted on a

battery test station (LAND) at different current densities with a voltage window from 0.02 V to 2.5 V vs Li^+/Li. Cyclic voltammograms (CV) curves were carried out on an electrochemical workstation (CHI660D, Chenhua Co.) between 0.02 to 2.5 V at different scan rates. Electrochemical impedance spectra (EIS) analysis in the frequency range from 100 kHz to 0.01 Hz was tested on the CHI660D electrochemical workstation.

Theoretical calculations: AIMD was performed with the CP2K package, within the generalized gradient approximation proposed by the Perdew-Burke-Ernzerhof (PBE). In order to add more oxygen-containing functional groups, we constructed a large three-layer structure of 21.2Å*21.2Å*32.2Å containing P (100), CoPPc and GO. The k point was taken as GAMMA point. And the vacuum layer thickness was 15Å. The $LiPF_6$ molecule was placed above the matrix. The hot bath was controlled by Canonical sampling through velocity rescaling (CSVR), and the system was simulated at 300K with NVT (canonical) ensemble for 5ps. Prior to the dynamic simulation, the structure was roughly optimized to reduce the mechanical problems of the initial structure. Additionally, the GO/P structure as the control group was also calculated as above. The Goedecker-Teter-Hutter (GTH) pseudopotentials, DZVP-MOLOPT-SR-GTH basis sets were used to describe the atoms. A plane-wave energy cut-off and relative cut-off of 400 Ry and 55 Ry were employed, respectively. The DFT-D3 method (46) was adopted to control the correction of Van der Waals (vdW) interaction. Mulliken charge analysis defined the atomic charge distribution. The software VESTA were used for visualization. Some input files were generated using Multiwfn software. The band structures, PDOS and electron density difference were conducted using the CASTEP module of Materials Studio software. All calculations were also performed within the framework of the generalized gradient approximation (GGA) in the form of PBE for the exchange-correlation functional.

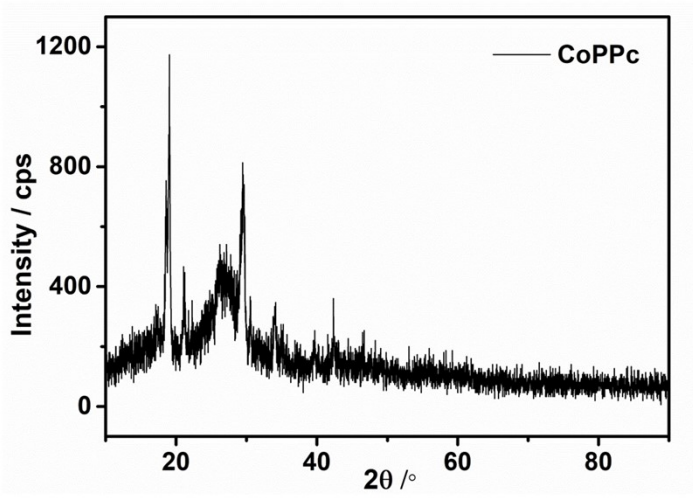

Fig. S1 XRD pattern of CoPPc.

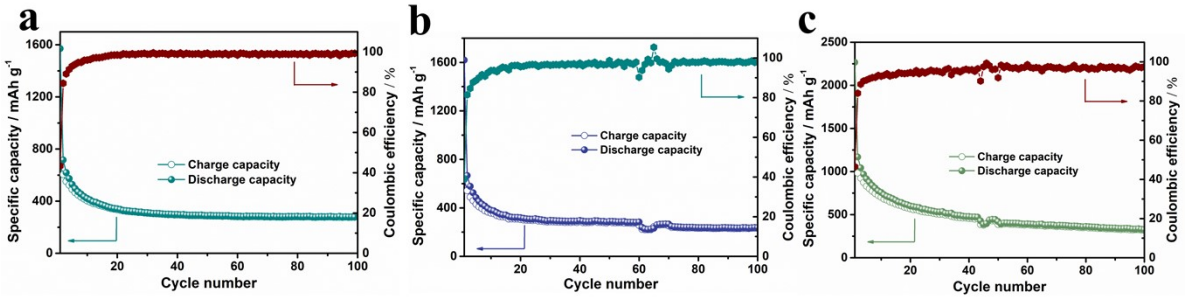

Fig. S2 Cycling performances of the (a) CoPPc, (b) GO and (b) CoPPc/GO electrodes.

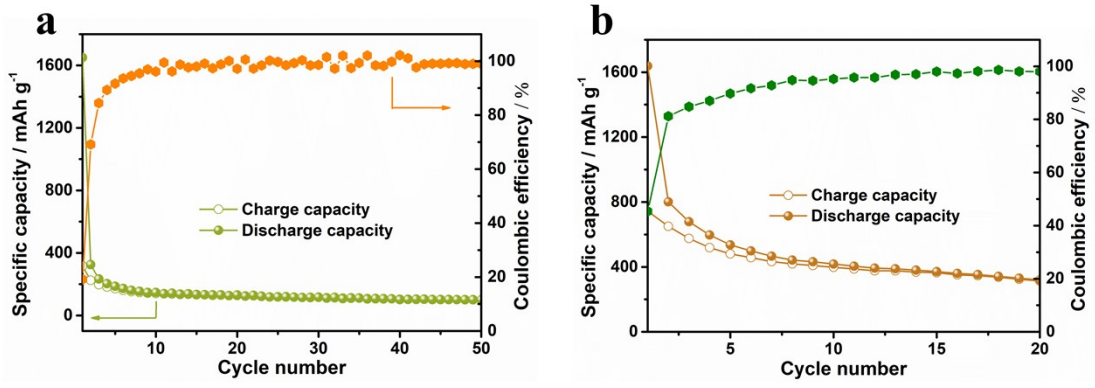

Fig. S3 Cycling performances of the (a) M-P/CoPPc and (b) M-P-CoPPc/GO electrodes.

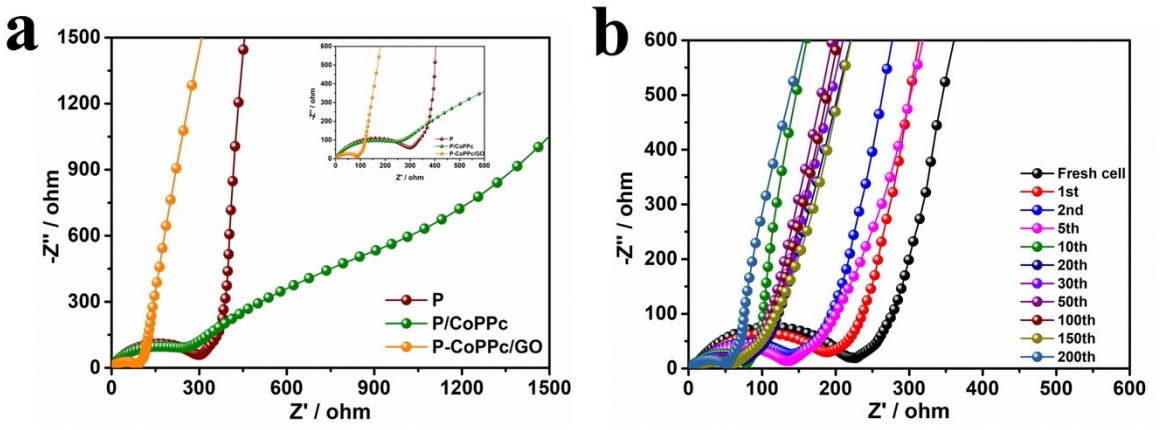

Fig. S4 (a) Nyquist plots of P, P/CoPPc and P-CoPPc/GO composites (inset: the magnified image of the Nyquist curves); (b) Nyquist plots taken from the P-CoPPc/GO electrode after the different cycles.

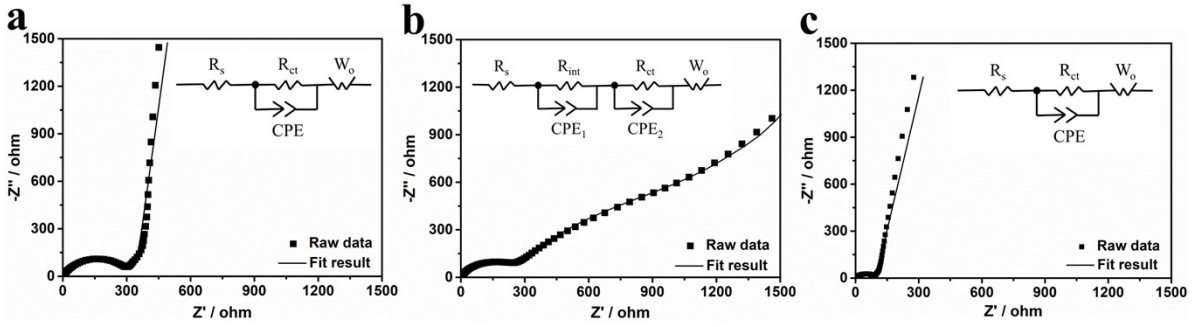

Fig. S5 Nyquist plots and equivalent circuits of different samples (a) P; (b) P/CoPPc; (c) P-CoPPc/GO composites.

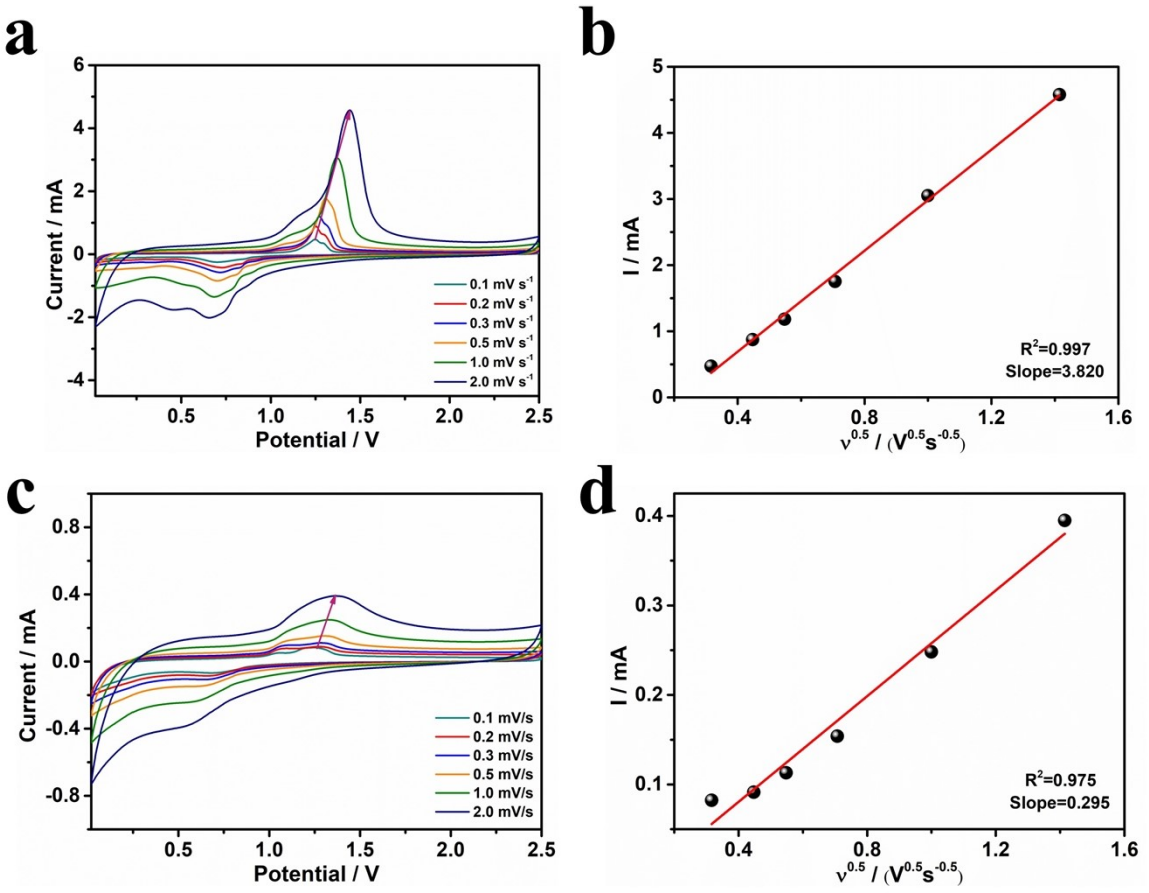

Fig. S6 (a) Cyclic voltammetry curves of P-CoPPc/GO composite at different scan rates; (b) The relationship of peak current (I) and square root of the scan rate ($\nu^{0.5}$); (c) Cyclic voltammetry curves of P/CoPPc composite at different scan rates; (d) The relationships of I and $\nu^{0.5}$.

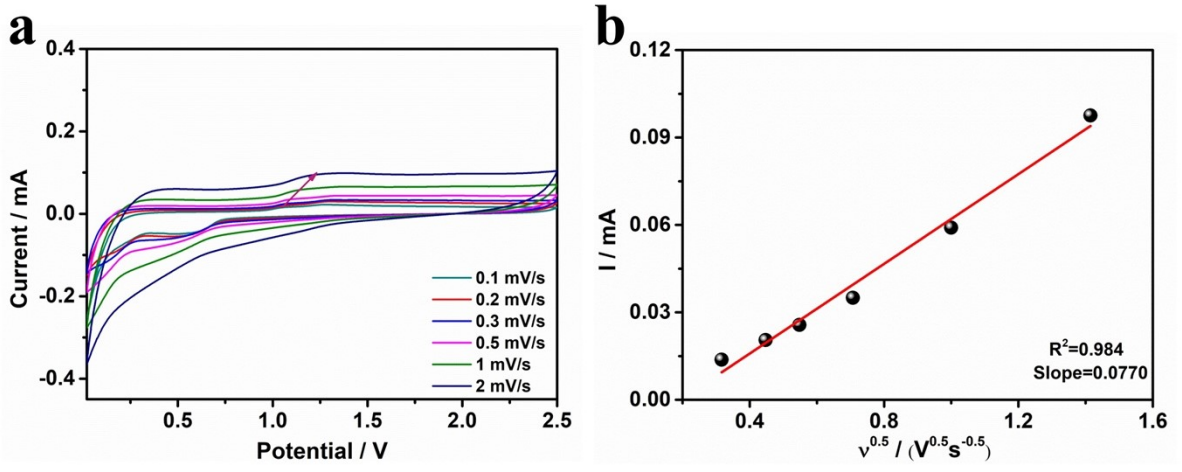

Fig. S7 (a) Cyclic voltammetry curves of P electrode at different scan rates; (b) The relationship of peak current (I) and square root of the scan rate ($\nu^{0.5}$).

The Li ions diffusion coefficient (D_{Li^+}) of samples could be calculated on basis of the CV results by the following Randles-Sevcik equation: [1-3]

$$I_P = (2.69*10^5)\, n^{1.5}\, AD^{0.5}Cv^{0.5} \qquad (1)$$

Where I_P is the peak current (mA), n corresponds to the number of electrons involved in the reaction, A is the area of anode electrode, D stands for the Li ions diffusion coefficient, C represents the concentration of Li ions in electrode, and ν is potential sweep rate. Besides, by plotting the relationship of peak current and square root of the scan rate, the Li ions diffusion coefficient (D_{Li^+}) of samples can be obtained through calculating, where the slope is displayed in **Figure** S4 and S5.

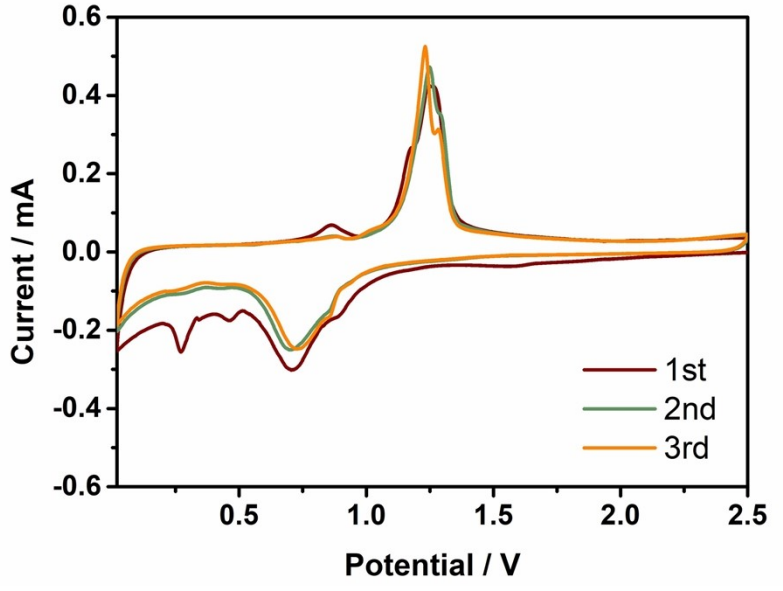

Fig. S8 Cyclic voltammetry curves of P-CoPPc/GO composite from the 1st to the 3rd cycle at a scan rate of 0.1 mV s^{-1}.

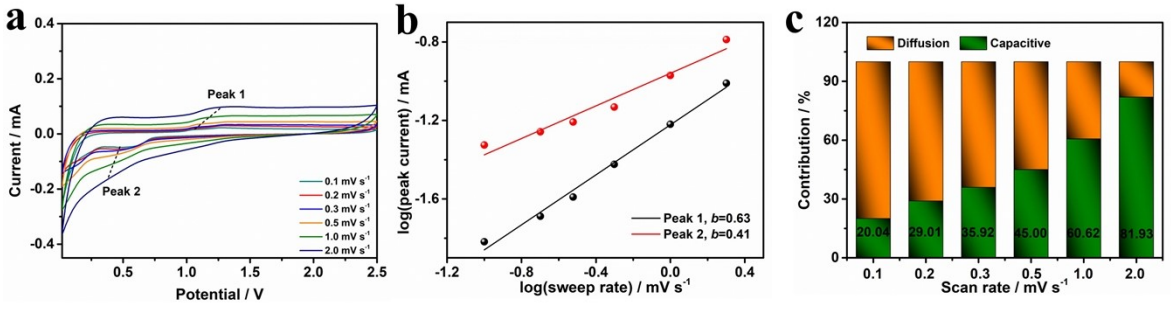

Fig. S9 (a) Cyclic voltammetry curves of P electrode at different scan rates; (b) The relationships between log (peak current) and log (sweep rate); (c) The contribution ratios of pseudocapacitive at different scan rates (P electrode).

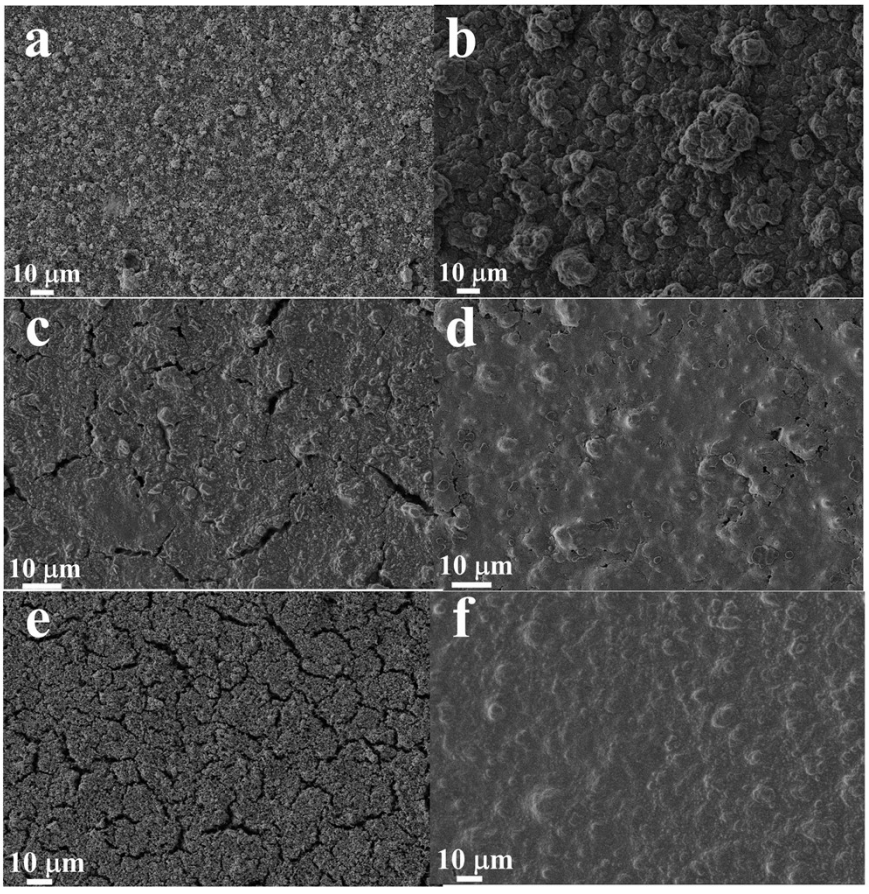

Fig. S10 The SEM images of different electrodes before and after cycling. (a) The pristine P electrode; (b) The P electrode after 20 cycles; (c) The pristine P/CoPPc electrode; (d) The P/CoPPc electrode after 20 cycles; (e) The pristine P-CoPPc/GO electrode; (f) The P-CoPPc/GO electrode after 20 cycles.

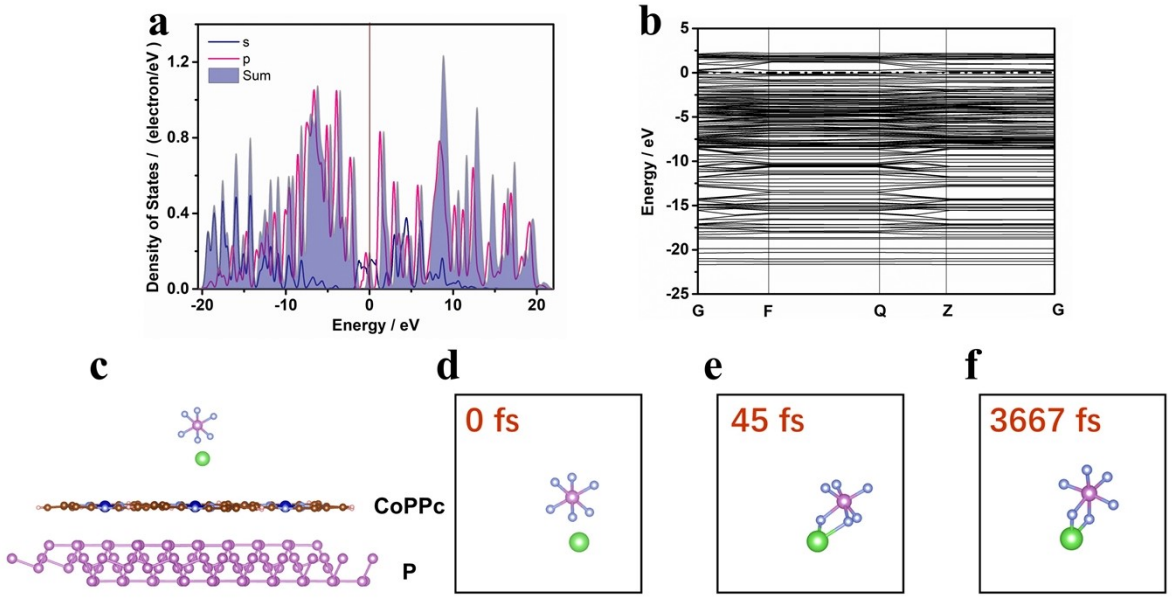

Fig. S11 (a) The partial density of states (PDOS) of GO; (b) The band structures of CoPPc/GO; (c) AIMD simulation of P/CoPPc illustrating the decomposition of $LiPF_6$ in electrolyte:(d) 0 fs, (e)45 fs and (f) 3667 fs.

Table S1. Comparison of the rate capabilities of our work with other phosphorus-based anode materials for LIBs reported previously

Materials	Current Density (mA g^{-1})	Capacity (mAh g^{-1})	Reference
P/rGO-C_3N_4	**200/2000**	**1800/780**	**[4]**
P@NPHPC	**200/1600**	**757/470**	**[5]**
BP@CNTs	**100/1500**	**2200/420**	**[6]**
P-C Film	**100/2000**	**1350/450**	**[7]**
P@Expanded-G	**100/2000**	**1500/470**	**[8]**
P-CoPPc/GO	**200/2000**	**2308.4/833.3**	**This work**

References

1 P. K. Dwivedi, S. K. Sapra, J. Pati, R. S. Dhaka, *ACS Appl. Energy Mater.* **2021**, *4*, 8076-8084.

2 J. Zhang, F. Wu, X. Dai, Y. Mai, Y. Gu, *ACS Sustainable Chem. Eng.* **2021**, *9*, 1741-1753.

3 T. L. Nguyen, T. N. Vo, V. D. Phung, K. Ayalew, D. Chun, A. T. Luu, Q. H. Nguyen, K. J. Kim, I. T. Kim, J. Moon, *C. Eng. J.* **2022**, *446,*137174.

4 W. Kong, J. Yu, X. Shi, J. Yin, H. Yang, Z. Wen, *J. Electrochem. Soc.* 2020, **167**, 060518.

5 Z. Du, W. Ai, C. Yu, Y. Gong, R. Chen, G. Sun and W. Huang, *Sci. China Mater.* 2019, **63**, 55–61.

6 Y. Zhang, L. Wang, H. Xu, J. Cao, D. Chen and W. Han, *Adv. Funct. Mater.* 2020, **30**, 2070074.

7 J. Ruan, T. Yuan, Y. Pang, X. Xu, J. Yang, W. Hu, C. Zhong, Z. Ma, X. Bi, S. Zheng, ACS Appl. Mater. Interfaces 2017, **9** 36261–36268.

8 J. Ruan, Y. Pang, S. Luo, T. Yuan, C. Peng, J. Yang and S. Zheng, *J. Mater. Chem. A*, 2018, **6**, 20804–20812.